Three-Dimensional Structure in Lipid Micelles of the Pediocin-like Antimicrobial Peptide Curvacin A[†,‡]

Helen Sophie Haugen, Gunnar Fimland, Jon Nissen-Meyer, and Per Eugen Kristiansen*

Department of Molecular Biosciences, University of Oslo, Pb. 1041 Blindern, 0316 Oslo, Norway

Received June 24, 2005; Revised Manuscript Received October 1, 2005

ABSTRACT: The 3D structure of the membrane-permeabilizing 41-mer pediocin-like antimicrobial peptide curvacin A produced by lactic acid bacteria has been studied by NMR spectroscopy. In DPC micelles, the cationic and hydrophilic N-terminal half of the peptide forms an S-shaped β-sheet-like domain stabilized by a disulfide bridge and a few hydrogen bonds. This domain is followed by two α-helices: a hydrophilic 6-mer helix between residues 19 and 24 and an amphiphilic/hydrophobic 11-mer helix between residues 29 and 39. There are two hinges in the peptide, one at residues 16−18 between the N-terminal S-shaped β-sheet-like structure and the central 6-mer helix and one at residues 26−28 between the central helix and the 11-mer C-terminal helix. The latter helix is the only amphiphilic/hydrophobic part of the peptide and is thus presumably the part that penetrates into the hydrophobic phase of target-cell membranes. The hinge between the two helices may introduce the flexibility that allows the helix to dip into membranes. The helix−hinge−helix structure in the C-terminal half of curvacin A clearly distinguishes this peptide from the other pediocin-like peptides whose structures have been analyzed and suggests that curvacin A along with the structural homologues enterocin P and carnobacteriocin BM1 belong to a subgroup of the pediocin-like family of antimicrobial peptides.

Many Gram-positive bacteria produce ribosomally synthesized antimicrobial peptides (AMPs),[1] generally termed bacteriocins. These peptides are usually membrane-permeabilizing and cationic and contain between 25 and 60 residues (*1*, *2*). AMPs with these characteristics are also produced by plants and animals, including humans, and are thus widely distributed in nature. AMPs produced by "food grade" lactic acid bacteria (LAB) have especially been the focus of extensive studies because of their potential application as nontoxic food preservatives and therapeutic agents for gastrointestinal infections in mammals. Nisin is an example of a LAB AMP that is approved in over 40 countries for use as a food additive (*3*).

One important group of AMPs produced by LABs is the pediocin-like peptides, also termed class IIa bacteriocins. More than 20 pediocin-like peptides have been characterized so far (*2*, *4*−*30*). They have anti-*Listeria* activity and kill target cells by permeabilizing the cell membrane (*31*, *32*). In their N-terminal region they all have a disulfide bridge and a common YGNGV/L sequence motif (see Figure 1). They have very similar amino acid sequences, especially in their cationic and hydrophilic N-terminal half. The sequences of their hydrophobic/amphiphilic C-terminal half are somewhat more diverse, and the peptides have as a consequence been grouped into three subgroups according to sequence similarities and differences in the C-terminal half (*5*, *33*; see also Figure 1).

The three-dimensional structures of peptides from each of the three subgroups have been analyzed by NMR spectroscopy (*34*−*36*). All of the peptides are unstructured in water but become structured when exposed to membrane-mimicking environments. Sakacin P and leucocin A belong to subgroups 1 and 2, respectively. In the presence of membrane-mimicking environments, both peptides form an N-terminal three-stranded antiparallel β-sheet-like structure that is stabilized by the disulfide bridge present in the N-terminal half of all pediocin-like AMPs (*34*, *36*). This N-terminal β-sheet-like region is in both peptides followed by a central amphiphilic α-helix and this in turn by a rather extended C-terminal tail that folds back onto the central α-helix, thereby creating a hairpin-like structure in the C-terminal half (*36*). There is a flexible hinge (at the conserved Asp/Asn17 in subgroup 1 and 2 peptides; Figure 1) between the β-sheet-like N-terminal and the hairpin-like C-terminal regions, and one thus obtains two domains that may move relative to each other (*36*). The cationic N-terminal β-sheet-like domain appears to mediate binding of

[†] This work was supported by the Norwegian Research Council and by University funding through EMBIO.

[‡] NMR structures, assignments, and constraints have been deposited in the Protein Data Bank (http://www.rcsb.org/pdb/) under ID code 2A2B.

* Corresponding author. E-mail: eugen@kjemi.uio.no. Phone: (+47) 22856609. Fax: (+47) 22854443.

[1] Abbreviations: AMPs, antimicrobial peptides; CD, circular dichroism; DPC, dodecylphosphocholine; DSS, 2,2-dimethyl-2-silapentane-5-sulfonate sodium salt; HSQC, hetronuclear single-quantum correlation spectroscopy; LAB, lactic acid bacteria; MALDI-TOF, matrix-assisted laser desorption time of flight; MRS broth, de Man Rogosa Sharp broth; NMR, nuclear magnetic resonance; NOE, nuclear Overhauser effect; NOESY, two-dimensional nuclear Overhauser correlation spectroscopy; PDB, Protein Data Bank; RMSD, root mean square deviation; TFE, 2,2,2-trifluoroethanol; TOCSY, total correlation spectroscopy.

10.1021/bi051215u CCC: $30.25
Published on Web 11/16/2005

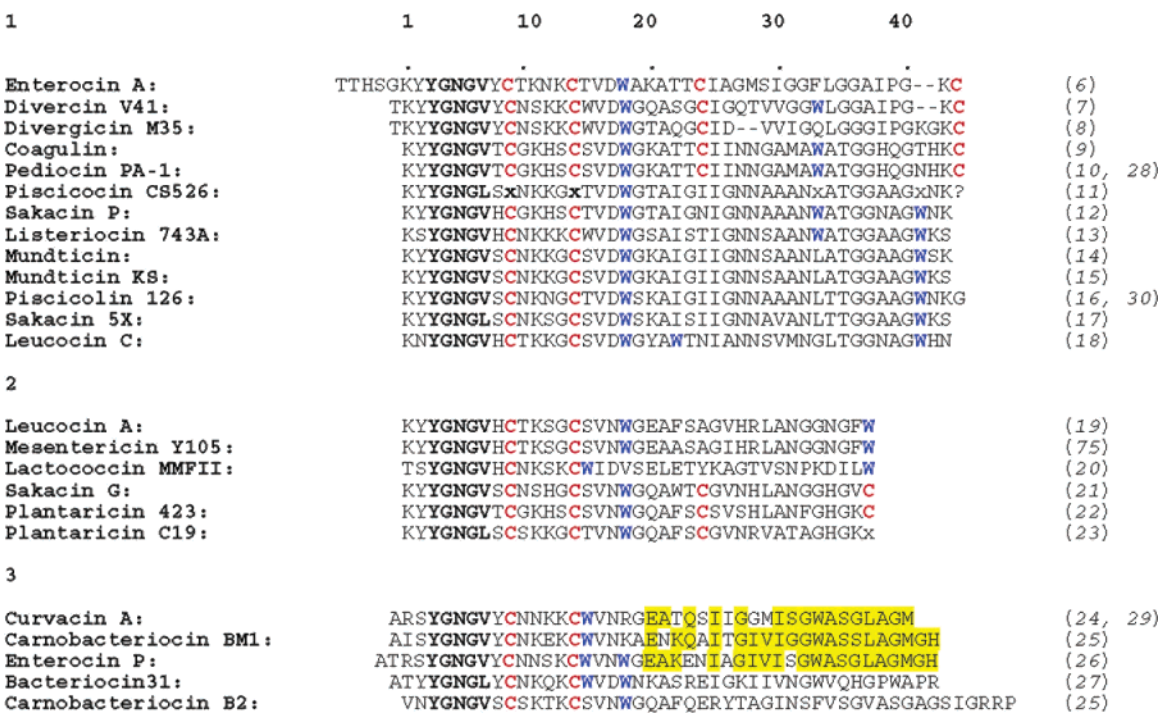

FIGURE 1: Alignment and grouping of 24 pediocin-like peptides. The common YGNGV/L is shown in bold face. The disulfide bridge-forming cysteines are shown in red, and tryptophans are shown in blue. The C-terminal residues in the vicinity of the second α-helix that are common for curvacin A, enterocin P, and carnobacteriocin BM1 are shown against a yellow background.

the pediocin-like peptides to the target-cell surface through electrostatic interactions (*37*, *38*), whereas the more hydrophobic/amphiphilic C-terminal hairpin-like domain penetrates into the hydrophobic part of the target-cell membrane, thereby mediating leakage through the membrane (*33*, *39*). The hinge apparently provides the structural flexibility that enables the C-terminal hairpin-like domain to dip into the hydrophobic part of the membrane (*33*).

The C-terminal hairpin-like structure is in some subgroup 1 and 2 peptides stabilized by a disulfide bridge between a C-terminal cysteine residue and a cysteine residue in the middle of the α-helix (*33*, *40*). Most of the peptides in subgroups 1 and 2, however, lack these two cysteine residues but instead contain a tryptophan residue near the C-terminal end of the peptide (Figure 1). This tryptophan residue is believed to position itself in the membrane−water interface along with the well-conserved central tryptophan residue (in position 18 in most subgroup 1 and 2 peptides; Figure 1), thereby stabilizing the hairpin-like structure in subgroup 1 and 2 peptides that lack the structure-stabilizing disulfide bridge in the C-terminal domain (*33*).

It is unclear whether the subgroup 3 peptides form the same overall three-dimensional structure as the subgroup 1 and 2 peptides. Structural analysis of the subgroup 3 peptide carnobacteriocin B2 revealed only a central α-helix, whereas the N-terminal half and the C-terminal tail lacked any clear structuring (*35*). The lack of structuring in the N-terminal half was unexpected, since a β-sheetlike structure is predicted on the basis of the high sequence similarity in this region in all pediocin-like peptides (Figure 1). The structure of the C-terminal half of subgroup 3 peptides is difficult to predict. Subgroup 3 peptides differ conceptually in their C-terminal sequence from subgroup 1 and 2 peptides. The subgroup 3 peptides lack both the hairpin-stabilizing disulfide bridge and the well-conserved hairpin-stabilizing tryptophan residue near the C-terminal end (Figure 1). The structure of the C-terminal half is of special interest, since this membrane-penetrating region is specifically recognized by the immunity protein that protects the AMP-producing bacteria from being killed by their own AMP (*39*, *41*). Moreover, the C-terminal half is also the major specificity determinant of the pediocin-like peptides, since hybrid peptides constructed by joining N- and C-terminal halves from different pediocin-like peptides have target-cell specificities similar to the peptide from which the C-terminal half is derived (*39*). In this study, we have analyzed the three-dimensional structure in lipid micelles of the subgroup 3 peptide curvacin A. Whereas the N-terminal half formed an S-shaped β-sheet-like structure, the C-terminal half formed a helix−hinge−helix structure that clearly differed from the hairpin-like C-terminal domain that appears to be typical for subgroup 1 and 2 peptides.

MATERIALS AND METHODS

Bacterial Strains and Culture Conditions. Lactobacillus sake NCDO 2714 (type strain) was used as the indicator strain in the activity assays and was cultured in MRS broth (Oxoid) at 30 °C. *Lactobacillus curvatus* LTH1174 (*24*) was used for production of curvacin A and was grown to the stationary phase in MRS broth at 30 °C.

Purification of Curvacin A. Curvacin A was purified to homogeneity from approximately 14 L of culture by applying the bacteria culture directly on a SP-Sepharose fast-flow cation exchanger (GE Healthcare; 500 mL of culture/5 mL of SP-Sepharose), washing the column with 100 mL 20 mM sodium phosphate (pH 6), followed by 30 mL of 0.15 mM NaCl in 20 mM sodium phosphate (pH 6), eluting the peptide with 40 mL of 1 M NaCl in 20 mM sodium phosphate (pH

6), and then purifying the peptide by reverse-phase chromatography using a Resource RPC column (GE Healthcare), all as described previously (*42*).

The primary structure and purity of the peptide were confirmed by mass spectrometry using a MALDI-TOF Voyager-DERP mass spectrometer (PerSeptive Biosystems) with α-cyano-4-hydroxycinnamic acid as matrix and by analytical reverse-phase chromatography using a μRPC SC 2.1/10 C2/C18 column (GE Healthcare) on the SMART chromatography system (GE Healthcare). Peptide concentrations were calculated from the absorbance at 280 nm using the molar extinction coefficient 13940 M^{-1} cm^{-1} (*43*). AMP activity was determined using a microtiter plate assay system, essentially as described earlier (*44*).

Circular Dichroism (CD) Spectroscopy. CD spectra were recorded by using a Jasco J-810 spectropolarimeter (Jasco International Co., Ltd., Tokyo, Japan) calibrated with ammonium D-camphor-10-sulfonate (Icatayama Chemicals, Tokyo, Japan). All of the measurements were performed at a constant peptide concentration of 0.15 mg/mL with DPC concentrations varying from 0 to 16 mM (CDN Isotopes, Quebec, Canada). Measurements were performed at 20−55 °C using a quartz cuvette (Starna, Essex, England) with a path length of 0.1 cm. Samples were scanned five times at 50 nm/min with a bandwidth of 1 nm and a response time of 1 s, over the wavelength range 190−260 nm. The data were averaged, and the spectrum of sample-free control was subtracted. The α-helical content of the various peptides was determined by application of spectral fitting methods in the CDpro package (*45*).

NMR Sample Preparation. For NMR structure elucidation, 6.8 mg of curvacin A was dissolved in 750 μL of 360 mM deuturated DPC (CDN Isotopes), a water solution with 10% D_2O (Cambridge Isotope Laboratories), and 0.1% trifluoroacetic acid (pH 2.8). The final concentration of the sample was 2.1 mM.

NMR Spectroscopy. The NMR spectra of curvacin A were obtained at 25, 30, and 35 °C on an 800 MHz Varian INOVA 800 NMR spectrometer with four channels and a 5 mm ^1H $\{^{13}C,^{15}N\}$ pfg probe. Natural abundance ^{15}N HSQC (*46*), TOCSY (*47*), and NOESY (*48*, *49*) experiments included in the BIOPACK were performed to assign the peptide. Spectra with mixing times of 48, 64, and 80 ms were acquired in the TOCSY experiment, and 100 and 150 ms were acquired in the NOESY experiment. Watergate water decoupling was applied in the HSQC, TOCSY, and NOESY experiments (*46*). A total of 1024K complex data points were obtained in the direct dimension and 512 in the indirect dimension of TOCSY and NOESY while 64 points were taken in the indirect dimension of the HSQC. A sine-bell function was applied to data, and it was zero-filled 2-fold prior to Fourier transformation. All postprocessing was done with the application of NMR Pipe (*50*), while spectral assignments and integration were done manually using SPARKY (T. D. Goddard and. D. G. Kneller, University of California, San Francisco). NOE restrictions were obtained from the structure assignment of the molecule. DSS was used as a chemical shift standard, and ^{15}N data were referenced using frequency ratios as described by Wishart et al. (*51*).

Restraints and Structure Calculation. The NOESY spectrum of the molecule was manually assigned using standard methods for analyzing NOESY and TOCSY spectra (*49*). A total of 567 NOE distance constraints were obtained after removal of the redundant NOE's, out of which 244 were interresidue and 323 were intraresidue NOE restraints. The 244 interresidue restraints were 24 long-range NOE restraints (more than four residues apart), 78 medium-range restraints (between two and four residues apart), and 142 sequential NOE's. ^{15}N chemical shift values were obtained from analysis of the HSQC spectrum. Dihedral angle restraints were obtained from the chemical shift values by the use of the TALOS program (*52*). A total of 36 torsion angle restraints were obtained. The structure was calculated and annealed by the application of the structure calculation program CYANA (*53*, *54*). Six hydrogen bonds were introduced in the final structure calculation, one between Glu21 and Ser25 and five in the C-terminal helix, between Ile31 and Ala35, Ser32 and Ser36, Gly33 and Gly37, Trp34 and Leu38, and Ala35 and Ala39. The standard CYANA structure calculation procedure was followed (*53*). The addition of hydrogen bonds did not change the overall fold of the structure but improved the backbone RMSD values.

A total of 100 structures were calculated out of which the 20 lowest energy structures were selected for further evaluation. The target function gave an average potential energy of $1.71 \times 10^{-1} \pm 9.43 \times 10^{-2}$ kJ mol^{-1}. The structures were visualized and RMSD values calculated with the MOLMOL program (*55*).

Table 1: Secondary Structure of Curvacin A Determined by CD Spectroscopy

	CONTINN/LL analysis		
DPC conc (mM)	% helix[a]	% β-sheet[b]	% turn
0	6	32	22
1	5	31	23
2	16	29	19
4	21	26	18
8	31	23	17
12	34	19	18
16	40	25	14

[a] Helix is the sum of $h(r) + h(d)$ values obtained from CONTINN/LL representing the right and distorted helical fraction. [b] β-Sheet is the sum of $s(r) + s(d)$ values obtained from CONTINN/LL representing the right and distorted β-sheet fraction.

RESULTS

Structural Analysis by CD Spectroscopy: α-Helical Structuring of Curvacin A upon Exposure to DPC Micelles. For CD and NMR structural analysis, curvacin A was purified to homogeneity by cation-exchange and reverse-phase chromatography to a yield of 0.5 mg/L of culture. Three different full spectrum methods [CONTINN/LL (*56*), CDSSTR (*57*), and SELCON 3 (*58*)] that belong to the CDpro package (*59*) were applied to determine the helical content from CD spectra. The three methods gave similar values for the α-helical content in curvacin A. CONTINN/LL gave, however, generally the smallest standard deviations and was consequently used to calculate the helical content presented in Table 1. Consistent with earlier studies on other pediocin-like peptides (*36*), the CD results revealed that curvacin A lacked helical structure in water but became structured, with an α-helical content between 16% and 40%, upon exposure to DPC micelles (Table 1). Increasing the temperature from

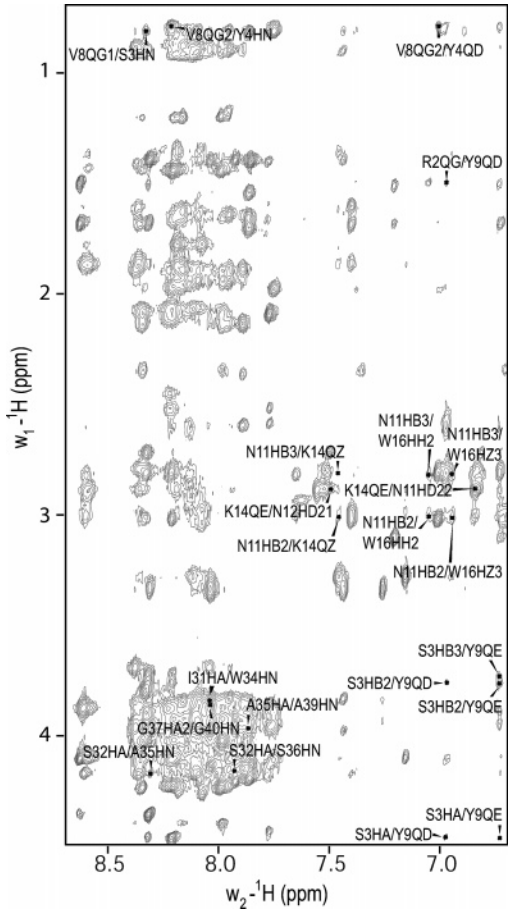

FIGURE 2: Fingerprint region of the NOESY spectrum of curvacin A in the presence of 100 mM DPC (150 ms mixing time). N-Terminal long-range and selected C-terminal intermediate-range NOE cross-peaks are identified.

20 to 55 °C resulted in only a slight reduction in the α-helical content (from 31% to 25% in 8 mM DPC), indicating that the helical structuring of curvacin A was not very temperature dependent in this temperature range.

Three-Dimensional Structure of Curvacin A Determined by NMR Spectroscopy. The fingerprint region of the NOE spectrum used in structure calculations is shown in Figure 2. The observed intramolecular NOE's and predicted torsion angles for curvacin A exposed to DPC micelles are shown in Figure 3A. According to structure predictions based only on chemical shift indexes, a series of four or more −1 indexes indicate an α-helix (*60*, *61*). This was observed from (and including) Ala22 to (and including) Ser25, indicating an α-helix in this region (Figure 3B). Similarly, an α-helix was predicted from (and including) Met30 to (and including) Ser36, as negative indexes were associated with all of these residues except Gly33 (Figure 3B). Analysis of the chemical shift data using the TALOS program (*52*) showed that most of the residues in the C-terminal half of curvacin A (from residue Gly29 and on) were in a coil/turn or α-helix type of structure. The reliable results obtained from this analysis are indicated with symbols for the ϕ and ψ values in Figure 3A. Triangles pointing up indicate that the ϕ and ψ are in agreement with what is expected for an α-helix. The observed NOE connectivities NN($i,i+2$), αN($i,i+3$) ,and αβ($i,i+3$) (Figure 3A) also clearly indicate the presence of a C-terminal helix stretching from (and including) Ile31 to (and including) Ala39 and a central helix stretching from (and including) Arg19 to (and including) residue Thr23.

Several medium- and long-range NOE's were found in the N-terminal part of curvacin A that indicated the folding of residues 2−4 close to residues 8 and 9 and, therefore, an N-terminal three-stranded antiparallel β-sheet, extending from (and including) Arg 2 to Trp16. These NOE's include, among others, Arg2 H_γ to Tyr9 H_α, Arg2 H_γ to Tyr9 H_β, Ser3 H_β to Tyr9 H_δ, Ser3 H_β to Tyr9 H_ϵ, Ser3 H_N to Val8 H_γ, Ser3 H_N to Tyr9 H_δ, Ser3 H_α to Tyr9 H_δ, Tyr4 H_N to Val8 H_γ, Tyr9 Q_δ to Trp16 H_ϵ, and Asn11 H_β to Cys15 H_N. The NOE's that go to the HN protons are shown in Figure 2. Two turns were found between Gly5 and Val8 and between Asn 11 and Lys14, respectively. The latter is stabilized by a disulfide bridge between Cys10 and Cys15.

The annealing macro that is a part of the program CYANA (*53*) was used to calculate 100 structures on the basis of the angular and distance restraints obtained from analysis of the NMR data. The 20 lowest energy structures were chosen for further investigation. In Figure 4A the structures are superimposed. The high freedom of movement of different regions relative to each other makes it difficult to observe any well-defined structure when the structures were superimposed over the entire length of curvacin A, the backbone (Cα, C, and N) RMSD value being 6.56 ± 1.88. An S-shaped structure was, however, clearly identified in the N-terminal half (residues 2−15) when the structures of that region of curvacin A were superimposed (Figure 4B), the backbone (Cα, C, and N) RMSD value being 1.99 ± 0.69. Although it was not possible based on the experimental data to assign a perfect β-sheet structure to this domain, the S-shape clearly indicates a β-sheet-like structure (*36*). The structure was a less perfect β-sheet than that found in the N-terminal domain of the subgroup 1 and 2 peptides sakacin P and leucocin A (*34*, *36*) but was much more ordered and well-defined than the unstructured N-terminal region of the subgroup 3 peptide carnobacteriocin B2 (*35*).

As discussed above, the chemical shift indexes and NOE interactions (Figure 3) indicate that there is an α-helix in the center of the peptide following the S-shaped β-sheet-like structure in the N-terminal half and an α-helix near the C-terminal end. Superimposing the structures over the two respective helical regions (Figure 4) reveals that the central helix stretches from (and including) Gly19 to (and including) Gln24, whereas the C-terminal helix extends from (and including) Gly29 to (and including) Ala39, the backbone (Cα, C, and N) RMSD values being 0.70 ± 0.35 and 0.18 ± 0.08, respectively. The lack of a well-defined structure when the structures were superimposed over the entire length of curvacin A (Figure 4A) indicates that the N-terminal S-shaped domain, the central helix, and the C-terminal helix may move relative to each other and that these three regions are consequently separated by hinge regions. The results of PROCHECK (*62*) on the structure of curvacin A showed that 67% of all residues were in the most favored, 19% were in additionally allowed, 10% were in generously allowed, and 3% were in disallowed regions. A cartoon drawing of the overall structure of curvacin A is shown in Figure 5, with arrows indicating the hinge separating the S-shaped N-terminal domain and the central 6-mer helix and the hinge separating the latter helix and the 11-mer C-terminal helix. It was not possible to determine an exact angle between the

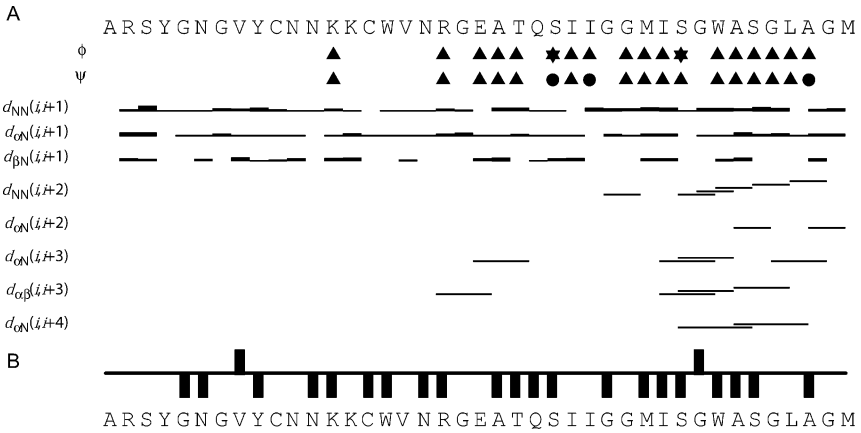

FIGURE 3: (A) Pattern of interresidue NOE's observed in the NOESY experiment (150 ms mixing time) with curvacin A in the presence of 100 mM DPC. The thickness of the lines shown are relative to the size of the NOE cross-peak intensities. The triangles indicate where TALOS found dihedral angle restraints that typically are for α-helices, stars indicate dihedral angles that can be for both α-helices and *β*-sheets, and circles indicate angles that are not found in either helices or *β*-sheets. (B) CSI indexes (*60*, *61*) observed by analysis of the Hα and N chemical shift values of curvacin A.

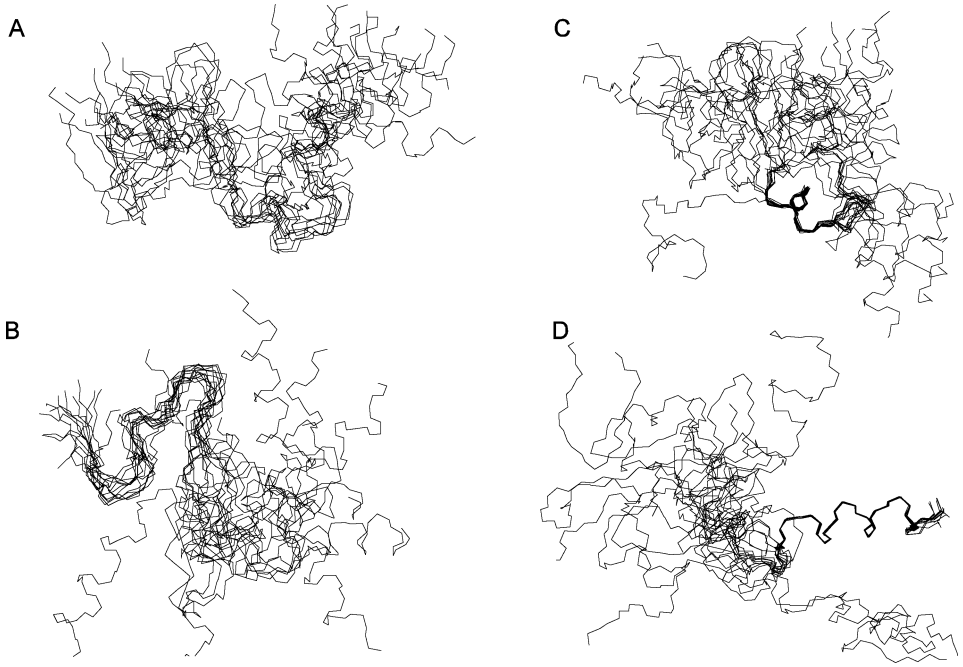

FIGURE 4: Backbone superposition of the 20 best structures of curvacin A. The peptide is shown with the N-terminal end pointing to the left and the C-terminal end to the right. The structures were superimposed over backbone atoms of the entire peptide (A), over residues 2−16 (B), over residues 19−24 (C), and over residues 29−39 (D).

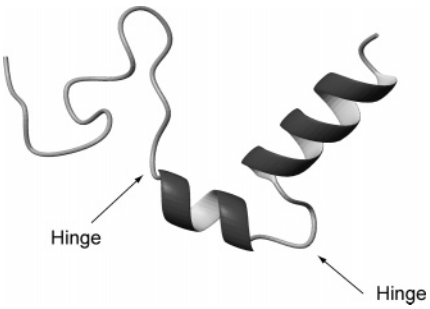

FIGURE 5: Cartoon drawing of curvacin A. Hinge regions between the S-shaped domain and first helix and between the first and second helix are indicated by arrows, and the orientation of the three regions relative to each other is consequently not well defined.

two helices and between the two domains due to the flexibility the two hinges introduce in the structure of the peptide.

DISCUSSION

By use of CD spectroscopy, a *β*-sheet content of 20−30% was observed in the subgroup 3 peptide curvacin A, and this was in reasonable agreement with what one would expect if its N-terminal domain forms a three-stranded antiparallel *β*-sheet-like structure as found in the subgroup 1 peptide sakacin P (*36*) and the subgroup 2 peptide leucocin A (*34*). The NMR experiments also revealed an S-shaped *β*-sheet-like structure in the N-terminal half of curvacin A when exposed to DPC micelles. This *β*-sheet-like structure was, however, not as distinct as that found in sakacin P (*36*) and leucocin A (*34*), but the N-terminal half was nevertheless much more structured than the N-terminal half of the subgroup 3 peptide carnobacteriocin B2 (*35*). One may speculate that the N-terminal half in all pediocin-like peptides adopts a well-defined structure, perhaps a more perfect three-stranded antiparallel *β*-sheet, when it interacts

with its docking site on the target-cell surface and that, in the absence of such a docking site, the region has some structural flexibility, varying somewhat from peptide to peptide and restricted to some extent by the conserved disulfide bond.

The C-terminal half is the helical region of curvacin A, as it is for all other pediocin-like peptides whose three-dimensional structure has been analyzed. The helical content in curvacin A determined by NMR analysis is in good agreement with the CD results that showed a helical content of about 40%. Superimposing the 20 lowest energy structures over various regions of curvacin A revealed a relative high freedom of movement of different regions relative to each other, and this was apparently due to two hinges. One hinge was in the vicinity of residues 16−18 between the N-terminal S-shaped β-sheet-like structure and the central 6-mer α-helix stretching from residue 19 to 24. This central helix is relatively hydrophilic (the only really nonpolar residue being an Ala22) and is thus expected to remain on or near the target-cell surface, as is the case for the cationic S-shaped β-sheet-like N-terminal domain. The second hinge appears to be between residues 26 and 28, and it separates the central α-helix and the 11-mer C-terminal α-helix stretching from residue 29 to 39. An Edmundson helical wheel presentation shows that an amphipilic helix might have been formed from Gly24 to Thr34. However, such a helix is unlikely since two Gly residues in a row (Gly28 and Gly29) would form a flexible region. The observed C-terminal α-helix is somewhat amphiphilic, the polar side consisting of Gly29, Ser32, Gly33, Ser36, and Gly37. The presence of this latter helix is in good agreement with the structure obtained upon modeling curvacin A (see Figure 4f in ref *63*). This helix is the only hydrophobic/amphiphilic part in curvacin A and is thus the only part that may penetrate into the hydrophobic phase of target-cell membranes. The hinge between the two helices may introduce the flexibility that enables the C-terminal helix to bend into the hydrophobic part of membranes.

This helix−hinge−helix structure in the C-terminal half of curvacin A clearly differs from the C-terminal hairpin-like structure present in the subgroup 1 and 2 peptides. Curvacin A and the other subgroup 3 peptides are in fact not expected to form the C-terminal hairpin-like structure, as they have neither the hairpin-stabilizing tryptophan residue found near the C-terminal end in most subgroup 1 and 2 peptides nor the hairpin-stabilizing disulfide bridge found in other subgroup 1 and 2 peptides. The helix−hinge−helix structure in the C-terminal half of curvacin A and the C-terminal hairpin-like structure present in the subgroup 1 and 2 peptides may nevertheless be functionally equivalent, as both structures constitute the part of pediocin-like peptides that penetrates into the target-cell membrane, thereby mediating leakage through the membrane. Moreover, they constitute the part that is specifically recognized by the four-helix bundle immunity protein that protects the peptide-producing bacteria from being killed by their own peptide (*39*, *41*, *64*), and they are the major target-cell specificity determinants of these peptides (*39*).

A chiral interaction with a target-cell receptor appears to be necessary for pediocin-like peptides to exert their antimicrobial activity, since the D-enantiomeric form of the pediocin-like peptide leucocin A is inactive (*65*). The fact that the membrane-penetrating C-terminal half is important in determining the target-cell specificity, combined with the observation that peptide fragments starting from the central hinge and going toward the C-terminal end inhibit pediocin-like peptides in a specific manner (*66*, *67*), suggests that this region of the C-terminal domain (i.e., the helical region) interacts with a receptor in the interface and/or hydrophobic region of the membrane (*65*). A protein complex that might act as a receptor is the membrane-bound mannose phosphotransferase system permease, as a subunit of this complex must apparently be expressed in order for cells to be sensitive to pediocin-like peptides (*68*−*73*). Results from recent activity studies with peptides that have been altered in the N-terminal domain suggest that the N-terminal three-stranded β-sheet-like domain associates with anionic membranes through ionic interactions and thereby positions itself in the membrane interface in a manner that allows the C-terminal domain to dip into the more hydrophobic part of the membrane and to engage in chiral interactions with membrane components (Fimland et al., submitted for publication).

The sequence similarities in the C-terminal half of curvacin A and the two subgroup 3 peptides enterocin P and carnobacteriocin BM1 (Figure 1) suggest that the two latter peptides are structurally similar to curvacin A. Immunity proteins discriminate pediocin-like peptides by specifically recognizing the peptides' C-terminal half (*39*). The fact that the immunity proteins for curvacin A, enterocin P, and carnobacteriocin BM1 have a much higher sequence similarity to each other than to the immunity proteins for other pediocin-like peptides (*74*) suggests that these three peptides have similar three-dimensional structures in their C-terminal half. Moreover, the fact that both the curvacin A immunity protein and the enterocin P immunity protein specifically recognize the C-terminal half of both curvacin A and enterocin P (but not other subgroup 1 and 2 peptides that were tested) (*74*) also indicates that curvacin A and enterocin P have similar three-dimensional structures in their C-terminal half. Also, earlier studies showing that curvacin A and enterocin P have similar target-cell specificities (*26*, *43*) suggest that these two peptides have similar structures in their C-terminal half, since this half is important in determining the target-cell specificity of pediocin-like peptides (*39*). Edmundson helical wheel analysis of carnobacteriocin BM1 and enterocin P shows that from residue 30 to 43 and from residue 26 to 44, respectively, they may form a C-terminal amphiphilic helix similar to that found in curvacin A. From residue 18 to 24 and from residue 21 to 24, respectively, they may also form a central polar helix as is found in curvacin A. The sequence alignments (Figure 1) do not show such a marked sequence similarity between curvacin A, carnobacteriocin B2, and bacteriocin 31 as between curvacin A, enterocin P, and carnobacteriocin BM1. We consequently suggest that subgroup 3 should presently be restricted to curvacin A, carnobacteriocn BM1, and enterocin P and that bacteriocin 31 and carnobacteriocin B2 thus should be transferred to a fourth subgroup.

ACKNOWLEDGMENT

We thank Dr. Gøran Karlson at the Swedish NMR Center in Gothenburg for letting us use the instruments.

SUPPORTING INFORMATION AVAILABLE

Chemical shift and NOE assignments. This material is available free of charge via the Internet at http://pubs.acs.org.

REFERENCES

1. Nissen-Meyer, J., and Nes, I. F. (1997) Ribosomally synthesized antimicrobial peptides: their function, structure, *Arch. Microbiol. 167*, 67−77.
2. Nes, I. F., Holo, H., Fimland, G., Hauge, H. H., and Nissen-Meyer, J. (2001) in *Peptide antibiotics, discovery, modes of action and application* (Dutton, H., McArthur, and Max, Eds.) Marcel Decker, New York.
3. Cleveland, J., Montville, T. J., Nes, I. F., and Chikindas, M. L. (2001) Bacteriocins: safe, natural antimicrobials for food preservation, *Int. J. Food Microbiol. 71*, 1−20.
4. Nissen-Meyer, J., Hauge, H. H., Fimland, G., Eijsink, V. G. H., and Nes, I. F. (1997) Ribosomally syntesized antimicrobial peptides produced by lactic acid bacteria: Their function, structure, biogenisis, and their mechanism of action, *Recent Res. Dev. Microbiol. 1*, 141−154.
5. Morisset, D., Berjeaud, J. M., Marion, D., Lacombe, C., and Frere, J. (2004) Mutational analysis of mesentericin Y105, an anti-*Listeria* bacteriocin, for determination of impact on bactericidal activity, in vitro secondary structure, and membrane interaction, *Appl. Environ. Microbiol. 70*, 4672−4680.
6. Aymerich, T., Holo, H., Havarstein, L. S., Hugas, M., Garriga, M., and Nes, I. F. (1996) Biochemical and genetic characterization of enterocin A from *Enterococcus faecium*, a new antilisterial bacteriocin in the pediocin family of bacteriocins, *Appl. Environ. Microbiol. 62*, 1676−1682.
7. Metivier, A., Pilet, M. F., Dousset, X., Sorokine, O., Anglade, P., Zagorec, M., Piard, J. C., Marion, D., Cenatiempo, Y., and Fremaux, C. (1998) Divercin V41, a new bacteriocin with two disulphide bonds produced by *Carnobacterium divergens* V41: primary structure and genomic organization, *Microbiology 144*, 2837−2844.
8. Tahiri, I., Desbiens, M., Benech, R., Kheadr, E., Lacroix, C., Thibault, S., Ouellet, D., and Fliss, I. (2004) Purification, characterization and amino acid sequencing of divergicin M35: a novel class IIa bacteriocin produced by *Carnobacterium divergens* M35, *Int. J. Food Microbiol. 97*, 123−136.
9. Le Marrec, C., Hyronimus, B., Bressollier, P., Verneuil, B., and Urdaci, M. C. (2000) Biochemical and genetic characterization of coagulin, a new antilisterial bacteriocin in the pediocin family of bacteriocins, produced by *Bacillus coagulans* I-4, *Appl. Environ. Microbiol. 66*, 5213−5220.
10. Marugg, J. D., Gonzalez, C. F., Kunka, B. S., Ledeboer, A. M., Pucci, M. J., Toonen, M. Y., Walker, S. A., Zoetmulder, L. C. M., and Vandenbergh, P. A. (1992) Cloning, expression, and nucleotide-sequence of genes involved in production of pediocin-PA-1, a bacteriocin from *Pediococcus acidilactici* Pac1.0, *Appl. Environ. Microbiol. 58*, 2360−2367.
11. Yamazaki, K., Suzuki, M., Kawai, Y., Inoue, N., and Montville, T. J. (2005) Purification and characterization of a novel class IIa bacteriocin, piscicocin CS526, from surimi-associated *Carnobacterium piscicola* CS526, *Appl. Environ. Microbiol. 71*, 554−557.
12. Tichaczek, P. S., Vogel, R. F., and Hammes, W. P. (1994) Cloning and sequencing of Sakp encoding sakacin-P, the bacteriocin produced by *Lactobacillus sake* Lth-673, *Microbiology 140*, 361−367.
13. Kalmokoff, M. L., Banerjee, S. K., Cyr, T., Hefford, M. A., and Gleeson, T. (2001) Identification of a new plasmid-encoded sec-dependent bacteriocin produced by *Listeria innocua* 743, *Appl. Environ. Microbiol. 67*, 4041−4047.
14. Bennik, M. H. J., Vanloo, B., Brasseur, R., Gorris, L. G. M., and Smid, E. J. (1998) A novel bacteriocin with a YGNGV motif from vegetable-associated *Enterococcus mundtii*: full characterization and interaction with target organisms, *Biochim. Biophys. Acta 1373*, 47−58.
15. Kawamoto, S., Shima, J., Sato, R., Eguchi, T., Ohmomo, S., Shibato, J., Horikoshi, N., Takeshita, K., and Sameshima, T. (2002) Biochemical and genetic characterization of mundticin KS, an antilisterial peptide produced by *Enterococcus mundtii* NFRI 7393, *Appl. Environ. Microbiol. 68*, 3830−3840.
16. Jack, R. W., Wan, J., Gordon, J., Harmark, K., Davidson, B. E., Hillier, A. J., Wettenhall, R. E. H., Hickey, M. W., and Coventry, M. J. (1996) Characterization of the chemical and antimicrobial properties of piscicolin 126, a bacteriocin produced by *Carnobacterium piscicola* JG126, *Appl. Environ. Microbiol. 62*, 2897−2903.
17. Vaughan, A., Eijsink, V. G. H., O'Sullivan, T. F., O'Hanlon, K., and van Sinderen, D. (2001) An analysis of bacteriocins produced by lactic acid bacteria isolated from malted barley, *J. Appl. Microbiol. 91*, 131−138.
18. Fimland, G., Sletten, K., and Nissen-Meyer, J. (2002) The complete amino acid sequence of the pediocin-like antimicrobial peptide leucocin C, *Biochem. Biophys. Res. Commun. 295*, 826−827.
19. Hastings, J. W., Sailer, M., Johnson, K., Roy, K. L., Vederas, J. C., and Stiles, M. E. (1991) Characterization of leucocin-A-Ual-187 and cloning of the bacteriocin gene from *Leuconostoc gelidum*, *J. Bacteriol. 173*, 7491−7500.
20. Ferchichi, M., Frere, J., Mabrouk, K., and Manai, M. (2001) Lactococcin MMFII, a novel class IIa bacteriocin produced by *Lactococcus lactis* MMFII, isolated from a Tunisian dairy product, *FEMS Microbiol. Lett. 205*, 49−55.
21. Simon, L., Fremaux, C., Cenatiempo, Y., and Berjeaud, J. M. (2002) Sakacin G, a new type of antilisterial bacteriocin, *Appl. Environ. Microbiol. 68*, 6416−6420.
22. Van Reenen, C. A., Chikindas, M. L., Van Zyl, W. H., and Dicks, L. M. T. (2003) Characterization and heterologous expression of a class IIa bacteriocin, plantaricin 423 from *Lactobacillus plantarum* 423, in *Saccharomyces cerevisiae*, *Int. J. Food Microbiol. 81*, 29−40.
23. Atrih, A., Rekhif, N., Moir, A. J. G., Lebrihi, A., and Lefebvre, G. (2001) Mode of action, purification and amino acid sequence of plantaricin C19, an anti-*Listeria* bacteriocin produced by *Lactobacillus plantarum* C19, *Int. J. Food Microbiol. 68*, 93−104.
24. Tichaczek, P. S., Nissen-Meyer, J., Nes, I. F., Vogel, R. F., and Hammes, W. P. (1992) Characterization of the bacteriocins curvacin A from *Lactobacillus curvatus* Lth1174 and Sakacin-P from *L. sake* Lth673, *Syst. Appl. Microbiol. 15*, 460−468.
25. Quadri, L. E. N., Sailer, M., Roy, K. L., Vederas, J. C., and Stiles, M. E. (1994) Chemical and genetic characterization of bacteriocins produced by *Carnobacterium piscicola* Lv17b, *J. Biol. Chem. 269*, 12204−12211.
26. Cintas, L. M., Casaus, P., Havarstein, L., Hernandez, P. E., and Nes, I. F. (1997) Biochemical and genetic characterization of enterocin P, a novel sec-dependent bacteriocin from *Enterococcus faecium* P13 with a broad antimicrobial spectrum, *Appl. Environ. Microbiol. 63*, 4321−4330.
27. Tomita, H., Fujimoto, S., Tanimoto, K., and Ike, Y. (1996) Cloning and genetic organization of the bacteriocin 31 determinant encoded on the *Enterococcus faecalis* pheromone responsive conjugative plasmid pYI17, *J. Bacteriol. 178*, 3585−3593.
28. Henderson, J. T., Chopko, A. L., and Vanwassenaar, P. D. (1992) Purification and primary structure of pediocin PA-1 produced by *Pediococcus acidilactici* Pac-10, *Arch. Biochem. Biophys. 295*, 5−12.
29. Holck, A., Axelsson, L., Birkeland, S. E., Aukrust, T., and Blom, H. (1992) Purification and amino acid sequence of sakacin A, a bacteriocin from *Lactobacillus sake* Lb706, *J. Gen. Microbiol. 138*, 2715−2720.
30. BhugalooVial, P., Dousset, X., Metivier, A., Sorokine, O., Anglade, P., Boyaval, P., and Marion, D. (1996) Purification and amino acid sequences of piscicocins V1a and V1b, two class IIa bacteriocins secreted by *Carnobacterium piscicola* V1 that display significantly different levels of specific inhibitory activity, *Appl. Environ. Microbiol. 62*, 4410−4416.
31. Moll, G. N., Konings, W. N., and Driessen, A. J. M. (1999) Bacteriocins: mechanism of membrane insertion and pore formation, *Antonie van Leeuwenhoek 76*, 185−198.
32. Chikindas, M. L., Garciagarcera, M. J., Driessen, A. J. M., Ledeboer, A. M., Nissen-Meyer, J., Nes, I. F., Abee, T., Konings, W. N., and Venema, G. (1993) Pediocin Pa-1, a bacteriocin from *Pediococcus acidilactici* Pac1.0, forms hydrophilic pores in the cytoplasmic membrane of target-cells, *Appl. Environ. Microbiol. 59*, 3577−3584.
33. Fimland, G., Eijsink, V. G. H., and Nissen-Meyer, J. (2002) Mutational analysis of the role of tryptophan residues in an antimicrobial peptide, *Biochemistry 41*, 9508−9515.

34. Gallagher, N. L. F., Sailer, M., Niemczura, W. P., Nakashima, T. T., Stiles, M. E., and Vederas, J. C. (1997) Three-dimensional structure of leucocin A in trifluoroethanol and dodecylphosphocholine micelles: Spatial location of residues critical for biological activity in type IIa bacteriocins from lactic acid bacteria, *Biochemistry 36*, 15062−15072.
35. Wang, Y. J., Henz, M. E., Gallagher, N. L. F., Chai, S. Y., Gibbs, A. C., Yan, L. Z., Stiles, M. E., Wishart, D. S., and Vederas, J. C. (1999) Solution structure of carnobacteriocin B2 and implications for structure−activity relationships among type IIa bacteriocins from lactic acid bacteria, *Biochemistry 38*, 15438−15447.
36. Uteng, M., Hauge, H. H., Markwick, P. R. L., Fimland, G., Mantzilas, D., Nissen-Meyer, J., and Muhle-Goll, C. (2003) Three-dimensional structure in lipid micelles of the pediocin-like antimicrobial peptide sakacin P and a sakacin P variant that is structurally stabilized by an inserted C-terminal disulfide bridges, *Biochemistry 42*, 11417−11426.
37. Chen, Y., Ludescher, R. D., and Montville, T. J. (1997) Electrostatic interactions, but not the YGNGV consensus motif govern the binding of pediocin PA-1 and its fragments to phospholipid vesicles, *Appl. Environ. Microbiol. 63*, 4770−4777.
38. Kazazic, M., Nissen-Meyer, J., and Fimland, G. (2002) Mutational analysis of the role of charged residues in target-cell binding, potency and specificity of the pediocin-like bacteriocin sakacin P, *Microbiology 148*, 2019−2027.
39. Johnsen, L., Fimland, G., and Nissen-Meyer, J. (2005) The C-terminal domain of pediocin-like antimicrobial peptides (class IIa bacteriocins) is involved in specific recognition of the C-terminal part of cognate immunity proteins and in determining the antimicrobial spectrum, *J. Biol. Chem. 280*, 9243−9250.
40. Fimland, G., Johnsen, L., Axelsson, L., Brurberg, M. B., Nes, I. F., Eijsink, V. G. H., and Nissen-Meyer, J. (2000) A C-terminal disulfide bridge in pediocin-like bacteriocins renders bacteriocin activity less temperature dependent and is a major determinant of the antimicrobial spectrum, *J. Bacteriol. 182*, 2643−2648.
41. Johnsen, L., Fimland, G., Mantzilas, D., and Nissen-Meyer, J. (2004) Structure−function analysis of immunity proteins of pediocin-like bacteriocins: C-terminal parts of immunity proteins are involved in specific recognition of cognate bacteriocins, *Appl. Environ. Microbiol. 70*, 2647−2652.
42. Uteng, M., Hauge, H. H., Brondz, I., Nissen-Meyer, J., and Fimland, G. (2002) Rapid two-step procedure for large-scale purification of pediocin-like bacteriocins and other cationic antimicrobial peptides from complex culture medium, *Appl. Environ. Microbiol. 68*, 952−956.
43. Eijsink, V. G., Skeie, M., P. H., M., Brurberg, M. B., and Nes, I. F. (1998) Comparative studies of class IIa bacteriocins of lactic acid bacteria, *Appl. Environ. Microbiol. 64*, 3275−3281.
44. Anderssen, E. L., Diep, D. B., Nes, I. F., Eijsink, V. G., and Nissen-Meyer, J. (1998) Antagonistic activity of *Lactobacillus plantarum* C11: two new two-peptide, *Appl. Environ. Microbiol. 64*, 2269−2272.
45. Sreerama, N., and Woody, R. W. (2000) Estimation of protein secondary structure from circular dichroism spectra: Comparison of CONTIN, SELCON, and CDSSTR methods with an expanded reference set, *Anal. Biochem. 287*, 252−260.
46. Sklenar, V., Piotto, M., Leppik, R., and Saudek, V. (1993) Gradient tailored water suppression for H-1-N-15 Hsqc experiments optimized to retain full sensitivity, *J. Magn. Reson., Ser. A 102*, 241−245.
47. Braunschweiler, L., and Ernst, R. R. (1983) Coherence transfer by isotropic mixing: application to proton correlation spectroscopy, *J. Magn. Reson. 53*, 521.
48. Jeener, J., Meier, B. H., Bachmann, P., and Ernst, R. R. (1979) Investigation of exchange processes by 2-dimensional NMR-spectroscopy, *J. Chem. Phys. 71*, 4546−4553.
49. Wuthrich, K. (1986) *NMR of proteins and nucleic acids*, Wiley-Interscience, New York.
50. Delaglio, F., Grzesiek, S., Vuister, G. W., Zhu, G., Pfeifer, J., and Bax, A. (1995) NMRpipe—a multidimensional spectral processing system based on Unix pipes, *J. Biomol. NMR 6*, 277−293.
51. Wishart, D. S., Bigam, C. G., Yao, J., Abildgaard, F., Dyson, H. J., Oldfield, E., Markley, J. L., and Sykes, B. D. (1995) H-1, C-13 and N-15 chemical-shift referencing in biomolecular NMR, *J. Biomol. NMR 6*, 135−140.
52. Cornilescu, G., Delaglio, F., and Bax, A. (1999) Protein backbone angle restraints from searching a database for chemical shift and sequence homology, *J. Biomol. NMR 13*, 289−302.
53. Guntert, P., Mumenthaler, C., and Wuthrich, K. (1997) Torsion angle dynamics for NMR structure calculation with the new program DYANA, *J. Mol. Biol. 273*, 283−298.
54. Guntert, P. (2004) in *Methods in molecular biology, protein NMR techniques* (Downing, A. K., Ed.) pp 353−378, Humana Press, Totowa, NJ.
55. Koradi, R., Billeter, M., and Wuthrich, K. (1996) MOLMOL: A program for display and analysis of macromolecular structures, *J. Mol. Graphics 14*, 51.
56. Sreerama, N., and Woody, R. W. (1994) Protein secondary structure from circular-dichroism spectroscopy—combining variable selection principle and cluster analysis with neural-network, ridge-regression and self-consistent methods, *J. Mol. Biol. 242*, 497−507.
57. Sreerama, N., and Woody, R. W. (1993) A self-consistent method for the analysis of protein secondary structure from circular dichroism, *Biophys. J. 64*, A170.
58. Johnson, W. C. (1999) Analyzing protein circular dichroism spectra for accurate secondary structures, *Proteins, Struct., Funct., Genet. 35*, 307−312.
59. Sreerama, N., and Woody, R. W. (2000) Analysis of protein CD spectra: Comparison of CONTIN, SELCON3, and CDSSTR methods in CDPro software, *Biophys. J. 78*, 334A.
60. Wishart, D. S., Sykes, B. D., and Richards, F. M. (1991) Simple techniques for the quantification of protein secondary structure by H-1-NMR spectroscopy, *FEBS Lett. 293*, 72−80.
61. Wishart, D. S., Sykes, B. D., and Richards, F. M. (1991) Relationship between nuclear-magnetic-resonance chemical shift and protein secondary structure, *J. Mol. Biol. 222*, 311−333.
62. Laskowski, R. A., MacArthur, M. W., Moss, D. S., and Thornton, J. M. (1993) PROCHECK: a program to check the stereochemcial quality of protein structures, *J. Appl. Crystallogr. 26*, 283−291.
63. Kaur, K., Andrew, L. C., Wishart, D. S., and Vederas, J. C. (2004) Dynamic relationships among type IIa bacteriocins: temperature effects on antimicrobial activity and on structure of the C-terminal amphipathic alpha helix as a receptor-binding region, *Biochemistry 43*, 9009−9020.
64. Sprules, T., Kawulka, K. E., and Vederas, J. C. (2004) NMR solution structure of ImB2, a protein conferring immunity to antimicrobial activity of the type IIa bacteriocin, carnobacteriocin B2, *Biochemistry 43*, 11740−11749.
65. Yan, L. Z., Gibbs, A. C., Stiles, M. E., Wishart, D. S., and Vederas, J. C. (2000) Analogues of bacteriocins: Antimicrobial specificity and interactions of leucocin A with its enantiomer, carnobacteriocin B2, and truncated derivatives, *J. Med. Chem. 43*, 4579−4581.
66. Fimland, G., Jack, R., Jung, G., Nes, I. F., and Nissen-Meyer, J. (1998) The bactericidal activity of pediocin PA-1 is specifically inhibited by a 15-mer fragment that spans the bacteriocin from the center toward the C terminus, *Appl. Environ. Microbiol. 64*, 5057−5060.
67. Saavedra, L., Minahk, C., Holgado, A. P. D., and Sesma, F. (2004) Enhancement of the enterocin CRL35 activity by a synthetic peptide derived from the NH2-terminal sequence, *Antimicrob. Agents Chemother. 48*, 2778−2781.
68. Ramnath, M., Beukes, M., Tamura, K., and Hastings, J. W. (2000) Absence of a putative mannose-specific phosphotransferase system enzyme IIAB component in a leucocin A-resistant strain of *Listeria* monocytogenes, as shown by two-dimensional sodium dodecyl sulfate-polyacrylamide gel electrophoresis, *Appl. Environ. Microbiol. 66*, 3098−3101.
69. Hechard, Y., Pelletier, C., Cenatiempo, Y., and Frere, J. (2001) Analysis of sigma(54)-dependent genes in *Enterococcus faecalis*: a mannose PTS permease (EIIMan) is involved in sensitivity to a bacteriocin, mesentericin Y105, *Microbiology 147*, 1575−1580.
70. Gravesen, A., Ramnath, M., Rechinger, K. B., Andersen, N., Jansch, L., Hechard, Y., Hastings, J. W., and Knochel, S. (2002) High-level resistance to class IIa bacteriocins is associated with one general mechanism in *Listeria* monocytogenes, *Microbiology 148*, 2361−2369.
71. Dalet, K., Cenatiempo, Y., Cossart, P., and Hechard, Y. (2001) A sigma(54)-dependent PTS permease of the mannose family is responsible for sensitivity of *Listeria* monocytogenes to mesentericin Y105, *Microbiology 147*, 3263−3269.
72. Ramnath, M., Arous, S., Gravesen, A., Hastings, J. W., and Hechard, Y. (2004) Expression of mptC of *Listeria monocytogenes* induces sensitivity to class IIa bacteriocins in *Lactococcus lactis*, *Microbiology 150*, 2663−2668.

73. Xue, J. F., Hunter, I., Steinmetz, T., Peters, A., Ray, B., and Miller, K. W. (2005) Novel activator of mannose-specific phosphotransferase system permease expression in *Listeria innocua*, identified by screening for pediocin AcH resistance, *Appl. Environ. Microbiol. 71*, 1283−1290.
74. Fimland, G., Eijsink, V. G. H., and Nissen-Meyer, J. (2002) Comparative studies of immunity proteins of pediocin-like bacteriocins, *Microbiology 148*, 3661−3670.
75. Fleury, Y., Dayem, M. A., Montagne, J. J., Chaboisseau, E., LeCaer, J. P., Nicolas, P., and Delfour, A. (1996) Covalent structure, synthesis, and structure−function studies of mesentericin Y 105(37), a defensive peptide from gram-positive bacteria *Leuconostoc mesenteroides*, *J. Biol. Chem. 271*, 14421−14429.

BI051215U